Zinc oxide-silver nanoparticles synthesized with plant extracts against Alternaria solani

Luis Gerardo Sarmiento-López¹ Joaquín Antonio Merlín-Trujillo² Hermila Trinidad García-Osuna² Luis Alfonso García-Cerda³ Ileana Vera-Reyes^{4,§}

- 1 Unidad de Investigación en Ambiente y Salud-Universidad Autónoma de Occidente. Unidad Regional Los Mochis, Sinaloa, México. CP. 81223. (iialuisg07@gmail.com).
- 2 Departamento de Fitomejoramiento-Universidad Autónoma Agraria Antonio Narro. Calz. Antonio Narro núm. 1923, Saltillo, Coahuila, México. CP. 25315. (merlintrujillojoa@gmail.com; hgosuna@gmail.com).
- 3 Departamento de Materiales Avanzados-Centro de Investigación en Química Aplicada. Blvd. Enrique Reyna Hermosillo 140, Saltillo, Coahuila, México. CP. 25294. (luis.garcia@ciqa.edu.mx). Departamento de Materiales Avanzados Centro de Investigación en Química Aplicada Saltillo Coahuila 25294 México luis.garcia@ciqa.edu.mx
- 4 Departamento de Biociencias y Agrotecnología-Centro de Investigación en Química Aplicada. Blvd. Enrique Reyna Hermosillo 140, Saltillo, Coahuila, México. CP. 25294.

Autor para la correspondencia: ileana.vera@ciga.edu.mx.

Antifungals, zinc nanoparticles, zinc-silver nanoparticles.

Abstract

Pathogen control has traditionally been addressed through the use of synthetic fungicides, generating adverse effects on the environment and agricultural production systems. In contrast, plant extracts contain bioactive compounds that modulate the development of phytopathogens. In addition, their synergistic effect with nanoparticles offers a promising and sustainable strategy for their application in agriculture. The objective was to use plant extracts from Flourensia cernua, Larrea tridentata and Lippia graveolens to synthesize zinc and zinc-silver nanoparticles and evaluate their antifungal effect against Alternaria solani. The nanoparticles synthesized at 400 °C from each extract had particle sizes less than 30 nm and an irregular hemispherical morphology, which was confirmed by X-ray diffraction and scanning electron microscopy techniques. The best inhibition effect and the greatest reduction in spore production of the strains were observed with the nanoparticles generated using 1 000 mg L⁻¹ of the L. graveolens extract, which inhibited 65% of growth and reduced spore production by 66% compared to the control. Adding silver to the nanoparticles significantly improved the ability to inhibit spore production, reaching 78% inhibition. These results suggested that zinc and zinc-silver nanoparticles, obtained from plant extracts, represent a promising alternative for the control of phytopathogenic fungi, and contribute to the reduction of the environmental impact associated with the excessive use of synthetic fungicides.

Keywords:

License (open-access): Este es un artículo publicado en acceso abierto bajo una licencia Creative Commons

elocation-id: e4040

Article



Introduction

Fungal diseases are responsible for losses in global agricultural production and they are one of the main threats to global food security. It is estimated that between 10 and 16% of global agricultural production is lost annually due to fungal infections, representing economic losses of more than 200 billion dollars (Sbai *et al.*, 2024). Phytopathogenic fungi not only affect yields, but also the quality of crops, which has a direct impact on the food supply and the global agricultural economy.

Among the most aggressive pathogens are species such as *Botrytis cinerea*, *Sclerotium rolfsii*, *Sclerotinia sclerotiorum*, *Alternaria alternata*, *Alternaria solani*, and *Fusarium* spp., which affect the productivity of high-value commercial crops, such as soybeans, beans, wheat, corn, rice, and tomatoes (Ahmad *et al.*, 2024; Kumar *et al.*, 2024). The control of these diseases has traditionally depended on the prolonged use of chemicals, pesticides, fungicides, and fertilizers, which, although effective, are now known to promote the emergence of resistant strains when overused, which compromises the effectiveness of treatments and forces farmers to resort to higher doses or the use of more toxic compounds, causing harm to humans and animals (Chandrasekaran and Paramasivan, 2024).

These issues emphasize the urgent need to explore more sustainable alternatives for fungal disease management in agriculture. Nanotechnology is an emerging area that provides innovative tools for crop protection against phytopathogenic fungi. Nanoparticles (NPs), specifically those of metals such as silver (Ag NPs), copper (Cu NPs), and zinc (Zn NPs), have demonstrated remarkable antimicrobial activity due to their unique properties derived from their nanometric size.

These NPs have a high surface-to-volume ratio, which gives them an exceptional ability to interact with fungal cells and release bioactive metal ions and cations, such as silver (Ag+) and zinc (Zn²⁺), which are responsible for their antimicrobial activity (Moradi *et al.*, 2021). These particles act through various mechanisms, including altering cell membrane permeability, generating reactive oxygen species (ROS), denaturing key proteins, and fragmenting DNA, leading to fungal cell death (Zhang *et al.*, 2024).

For example, in a recent study, Chen *et al.* (2022) showed that the application of copper nanoparticles (Cu NPs) confers resistance in tobacco plants against *Phytophthora nicotianae* infection by increasing the intracellular concentration of ROS and activating antioxidant enzymes. Likewise, studies conducted by Guilger-Casagrande and de Lima (2021) showed that the application of zinc nanoparticles (Zn NPs) inhibited the growth of *Fusarium equiseti* both under *in vitro* conditions and in *S. lycopersicum* crops under field conditions, possibly through ion exchange between nanoparticles and fungal cells, which alters their ionic balance, reducing the growth of the pathogen.

In addition to their direct action on pathogens, Ag NPs and Zn NPs can inhibit the formation of fungal biofilms, multicellular structures highly resistant to traditional fungicides, which improves their ability to eradicate infections in various agricultural crops (Rosenberg *et al.*, 2020). Interestingly, plant extracts, rich in bioactive compounds such as flavonoids, alkaloids, terpenoids, and phenols, act as stabilizers and enhancers of the antimicrobial properties of NPs.

Several studies have shown that plant extracts have a synergistic action with NPs, enhancing their antimicrobial effects in pathogens of agricultural importance, such as *Fusarium oxysporum*, *Colletotrichum gloeosporioides* and *Alternaria alternata* (Ali *et al.*, 2020). This combination of plant extracts with metal nanoparticles not only increases the efficiency of fungal disease control but also reduces environmental impact, as it is a greener and less toxic option compared to traditional methods that use synthetic compounds.

This study aimed to evaluate the synthesis of zinc oxide (ZnO NPs) and zinc oxide-silver (ZnO/Ag NPs) nanoparticles in synergy with plant extracts of *Flourensia cernua*, *Lippia graveolens*, and *Larrea tridentata*, and analyze their antifungal potential against *Alternaria solani* by *in vitro* tests.



Materials and methods

Plant material

Leaves and stems of *Flourensia cernua* D. C. (tarbush), *Lippia graveolens* HBK (Mexican oregano), and *Larrea tridentata* D. C. (creosote bush) were collected in the municipalities of Arteaga and Saltillo, Coahuila, during spring-summer 2021. The plant material was dried at a temperature of 70 °C for 24 h. Subsequently, the material was pulverized with a blender and stored in plastic bags in darkness in a place free of humidity until it was used as a raw material in the preparation of extracts used in the synthesis of nanoparticles.

Preparation of the aqueous extract

The extraction of the secondary metabolites from the three plant samples followed the methodology proposed by Méndez-Andrade *et al.* (2022): 10 g of the sample was taken, and a decoction method was performed at 60 °C for 1 h. Subsequently, the extract was filtered using filter paper to remove plant residues, collecting the supernatant. A second filtration was performed using a 22-micron porous filter funnel, collecting the filtrate, which was stored at 4 °C until use. The extract was prepared fresh and not stored for more than seven days to prevent degradation of the bioactive compounds.

Nanoparticle synthesis

The preparation was carried out according to the methodology reported by Muñoz-Ordoñez (2020). A 0.5 M zinc nitrate solution was prepared and mixed with the aqueous plant extract described above. The mixture was kept at 90 °C in constant stirring until a paste was obtained (the reaction time was less than 30 min). To obtain the ZnO/Ag NPs, silver nitrate was added to the zinc nitrate solution at 1% (w/w). The paste obtained was left to cool and transferred to a porcelain crucible to leave at 80 °C for 12 h.

The samples were then heat-treated at 400 °C for 1 h in a muffle furnace. The X-ray diffraction (XRD) patterns of the nanoparticles (NPs) were obtained using a Rigaku Ultima IV diffractometer with a CuK# radiation source, operated at 44 mA and 40 kV, in a scanning range of 10 to 80° on a 2# scale, at a speed of 0.02° s⁻¹. The crystalline phases present in the sample were identified by comparing the patterns obtained with the standard patterns of the International Centre for Diffraction Data (ICDD) database.

The crystallite size was determined using Scherrer's equation (Cullity, 1956) with the diffraction patterns obtained from each sample, using the Jade 6 software. In addition, the morphology of the nanoparticles was analyzed using scanning electron microscopy (SEM).

Antifungal activity

To evaluate the antifungal activity of zinc oxide (ZnO NPs) and zinc oxide-silver (ZnO/Ag NPs) nanoparticles against *A. solani*, the poisoned medium methodology described by Vera-Reyes *et al.* (2019) was used. In this study, the following concentrations were used: 0, 150, 250, 500 and 1 000 mg L⁻¹. Potato dextrose agar (PDA) medium was prepared with malt extract and yeast extract and was autoclaved at 121 °C for 15 min.

Simultaneously, a solution of nanoparticles dissolved in 10 ml of sterile distilled water was prepared and subjected to a sonication process in three 15-minute cycles. After sterilizing the PDA medium, the solution of previously sonicated nanoparticles was added, and this was stirred briefly to homogenize the mixture with the medium and then emptied into Petri dishes for later use in antifungal assays.

To establish the assay, the fungi were inoculated with explants in the media and incubated at 27 °C for 10 days. The parameter evaluated was the radial growth diameter, which was measured with a

vernier to calculate the percentage of inhibition using the formula described by Orberá-Ratón *et al.* (2009). To quantify the effect on the production of fungal spores, the procedure described by Bustillo (2010) was followed. The assays were conducted in triplicate and two independent experiments were conducted.

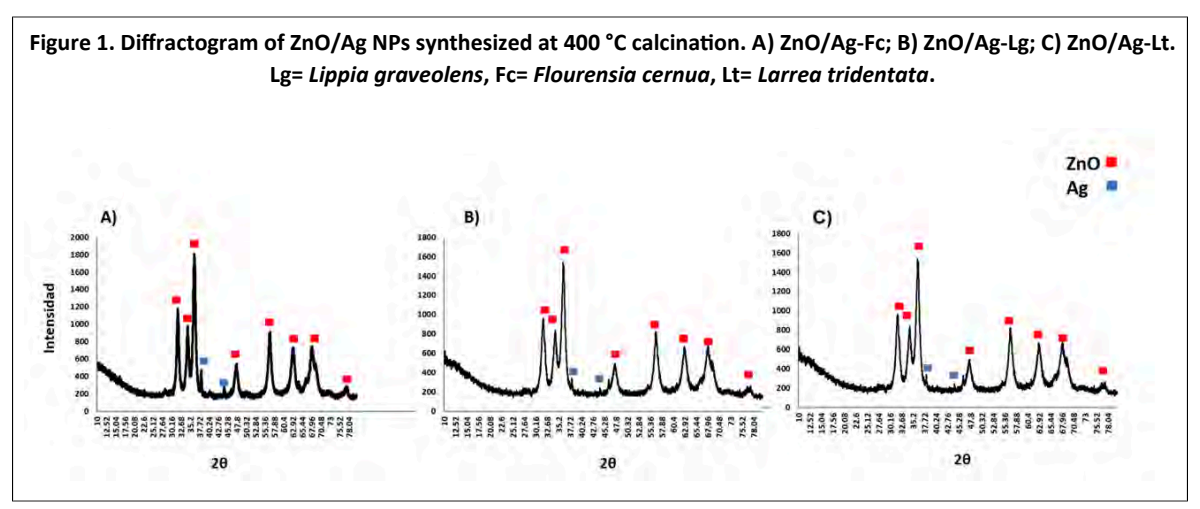
Statistical analysis

The experimental data was processed to calculate the mean and standard deviation. The data used in the one-way analysis of variance (Anova) passed the normality test, which was verified by the Shapiro-Wilk test. For the statistical comparison between the treatments, Tukey's test was used, considering a significance level of p< 0.05. Statistical analyses were performed using GraphPad Prism software (version 6.00; GraphPad, La Jolla, CA, USA).

Results and discussion

Characterization of nanoparticles by XRD

Figure 1 shows the diffraction pattern of the ZnO/Ag NPs, where the characteristic peaks of ZnO, previously discussed, were observed. In addition, it is possible to observe additional reflections corresponding to the presence of silver, located at 38.12°, 44.3°, and 64.46°, associated with the crystalline planes (111), (200), (220) and (311), respectively, which are characteristic of the metallic silver phase with a face-centered cubic (FCC) crystalline structure, according to JCPDS reference card No. 04-0783.



The detection of these peaks confirms the successful incorporation of Ag into the ZnO matrix, suggesting the formation of a heterostructured nanocomposite. This combination can enhance the antimicrobial properties of the material, as silver is recognized for its ability to generate reactive oxygen species (ROS) and disrupt bacterial cellular function by interacting with proteins and nucleic acids (Chen *et al.*, 2022; Zhang *et al.*, 2024).

In addition, the synergy between ZnO and Ag can enhance the photocatalytic and antibacterial activity of the nanomaterial due to the efficient transfer of electrons at the ZnO/Ag interface, reducing electron-hole pair recombination and increasing free radical generation (Al-Gaashani *et al.*, 2023).

The results show the formation of ZnO/Ag nanocomposites, due to the presence of diffraction peaks corresponding to two phases. The main one was indexed as ZnO with a hexagonal structure (JCPD No. 36-1451), while the other corresponded to a metallic Ag with a face-centered cubic structure (JCPDS No. 04-0783). The diffraction patterns confirm the crystalline nature of the composite material, and since no shifts were observed in the characteristic peaks of ZnO, it is inferred that Ag does not substitute Zn²⁺ ions in the crystal lattice of the oxide.

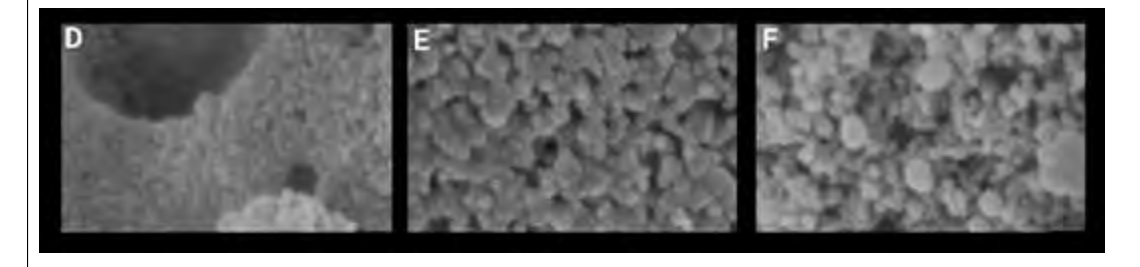


This indicates that both compounds coexist as individual phases, without forming a solid solution, which is consistent with what was reported by Meng *et al.* (2013). The presence of Ag as an independent phase suggests that silver NPs are deposited on the surface of ZnO or heterogeneously distributed in the matrix, which may favor the synergistic interaction between both materials.

According to Georgekutty *et al.* (2008), this configuration improves the photocatalytic and antimicrobial activity of the nanocomposite, as silver acts as an electron capture center, reducing the recombination of electron-hole pairs in ZnO, which increases the efficiency in the generation of reactive oxygen species (ROS). This synergy enhances the biocide applications of the material, which makes it promising for the control of plant pathogens.

The morphology of the ZnO and ZnO/Ag nanoparticles synthesized from the *L. graveolens*, *L. tridentata*, and *F. cernua* extracts was obtained by using scanning electron microscopy (SEM), as shown in Figure 2. The ZnO NPs synthesized with *L. graveolens* extract exhibited agglomeration on the surface and irregular-circular morphology and presented size variations within the agglomerates of approximately 20 nm.

Figure 2. SEM Micrograph of ZnO+Ag1% nanoparticles assisted with different plant extracts. D) ZnO/Ag-Lt; E) ZnO-Fc; F) ZnO/Ag-Fc. Lg= Lippia graveolens, Lt= Larrea tridentata, Fc= Flourensia cernua.



On the other hand, the addition of silver to zinc oxide in the ZnO/Ag NPs synthesized with *L. graveolens* (Figure 2), did not generate changes in morphology or a decrease in agglomeration on the surface of the NPs. On the other hand, in the micrograph obtained for the ZnO NPs synthesized with *L. tridentata* (Figure 2), the NPs showed greater uniformity in morphology, being mostly spherical, grouped in agglomerations, which indicates size variation within the agglomeration.

Distinctively, the addition of silver to zinc oxide in the *L. tridentata* extract presents a difference in the morphology of NPs; two shapes are observed: flat-rectangular and spherical (Figure 2D). On the other hand, the micrography of the NPs generated with ZnO-*F. cernua* obtained a spherical morphology with the presence of agglomerations (Figure 2E); regarding the ZnO/Ag NPs generated with *F. cernua* extract, they have a spherical shape (Figure 2F).

The results obtained through SEM, using the extracts of *L. graveolens*, *L. tridentata*, and *F. cernua* as reducing agents in the synthesis of ZnO and ZnO/Ag NPs, are consistent with what has been reported in the literature. Ahmad *et al.* (2020) described that ZnO NPs synthesized with *Eucalyptus globulus* extract presented a spherical morphology with an average size of 40-50 nm, observed by TEM.

SEM micrographs show a clear agglomeration of NPs on the surface of the analyzed samples, suggesting a similar effect to that described in the literature for green synthesis. This tendency to agglomeration can be attributed to the presence of residual bioactive compounds from plant extracts, such as flavonoids, tannins, and polyphenols, which can act as capping agents or stabilizers, favoring the interaction between particles (Anwar *et al.*, 2019).

Although agglomeration may reduce the specific surface area exposed, some studies have indicated that the formation of aggregates in ZnO/Ag NPs may increase antimicrobial activity due to the controlled release of metal ions and the ability to damage bacterial cell membranes by direct contact mechanisms (Shireen-Akhter *et al.*, 2024).



In vitro antagonism against Alternaria solani

The growth evaluation of *Alternaria solani* was performed when it reached 100% mycelial growth, which was seven days after seeding. Table 1 shows the results obtained by the different treatments of Ns ZnO and ZnO/Ag on mycelium growth. The antagonistic effect of NPs correlates with the increase in their concentration, so the highest percentage of inhibition of mycelial growth was observed at higher doses (1 000 mg L⁻¹), as shown in Table 1.

Table 1. Percentage of inhibition of radial growth of *Alternaria solani* due to the effect of zinc oxide and zinc oxide/ silver nanoparticles synthesized with different plant extracts.

Type of nanoparticles	Concentration (mg L-1)				
	150	250	500	1000	
ZnO-Lg	26.1 ±1.5 ^{dc}	47.63 ±1.26 ^a	57.73 ±0.85 ^a	65.22 ±0.5 ^a	
ZnO-Lt	27.81 ±2.02 ^{bcd}	51.46 ±0.65 ^a	60.46 ±0.7 ^a	63.87 ±0.68 ^a	
ZnO-Fc	22.49 ±1.84 ^d	42.28 ±1.64 ^b	60.33 ±0.29 ^a	62.06 ±0.78 ^a	
Added with silver at 1%					
ZnO/Ag-Lg	40.03 ±0.42 ^a	47.91 ±0.7 ^a	51.21 ±0.76 ^b	56.38 ±0.96 ^b	
ZnO/Ag-Lt	31.86 ±0.32bc	37.54 ±0.86°	41.45 ±0.88d	44.87 ±0.22°	
ZnO/Ag-Fc	33.85 ±1.06 ^{ab}	38.05 ±0.65 ^{bc}	45.13 ±0.86°	44.04 ±0.59°	

The data represents the mean \pm standard deviation of three independent experiments. Different letters indicate a significant difference according to Tukey's test (p< 0.05). Lg= *Lippia graveolens*, Lt= *Larrea tridentata*, Fc= *Flourensia cernua*.

ZnO-Lg NPs managed to inhibit 50% of radial growth from 500 mg L $^{-1}$, reaching 65.22 ±0.5% at the maximum concentration evaluated. On the other hand, ZnO NPs with *L. tridentata* extract (ZnO-Lt) managed to inhibit 50% of radial growth at 250 mg L $^{-1}$, and inhibition increased to 63.87 ±0.68% at 1 000 mg L $^{-1}$ (Table 1). On the other hand, ZnO NPs synthesized with *F. cernua* extract (ZnO-Fc) reached 60.33 ±0.29% radial growth inhibition at a concentration of 500 mg L $^{-1}$ and increased their inhibitory effect by 2% more at a concentration of 1 000 mg L $^{-1}$.

The best inhibitory effect of *A. solani* was obtained with ZnO-Lg NPs at the maximum concentration (1 000 mg L⁻¹). It should be noted that the inhibition effect at the maximum concentration used does not present significant differences between the extracts used, since all the synthesized ZnO NPs presented a radial inhibition effect of more than 60%.

Nevertheless, the addition of silver to the ZnO NPs was shown to increase the antifungal capacity of the NPs at low concentrations (150 and 250 mg L $^{-1}$). ZnO/Ag-Lg NPs at 150 mg L $^{-1}$ increased antifungal capacity by 54.4% (40.03 ±0.42) compared to ZnO NPs without silver (ZnO-Lg); however, at the higher concentrations evaluated, there was no increase in inhibition due to the addition of silver. In the case of ZnO/Ag-Lt NPs, they increased the antifungal capacity by 14.5% at 150 mg L $^{-1}$, but when the concentration increased, it had a negative behavior, decreasing the antifungal effect of ZnO/Ag-Lt NPs by 29.7% at 1 000 mg L $^{-1}$ compared to ZnO-Lt NPs.

A similar behavior was observed in ZnO/Ag-Fc NPs, which only increased antifungal capacity at low concentrations (150 mg L⁻¹), and when the concentration of NPs in the medium increased, this capacity decreased. The results obtained in this study are consistent with what has been reported in the literature regarding the inhibitory effect of ZnO NPs on *Alternaria solani*. Abdelhakim *et al.* (2020) described that ZnO NPs synthesized with *Alternaria tenuissima* showed significant antifungal activity against *A. solani*, demonstrating a dose-dependent effect, where inhibition began at 200 mg L⁻¹ and the largest diameter of the inhibition zone was reached at 400 mg L⁻¹.

Similarly, Ali *et al.* (2020) reported that ZnO NPs obtained from Neem extract were able to reduce the growth of *A. solani* by 45%, confirming their antifungal capacity. In general, the application of ZnO NPs obtained from the *L. graveolens*, *L. tridentata*, and *F. cernua* extracts demonstrated concentration-dependent fungal inhibition, with a greater effect observed as the dose of NPs



increased. The best result was obtained with ZnO NPs synthesized with *L. graveolens* extract, achieving the most significant inhibition at 1 000 mg L⁻¹.

This result could be attributed to the higher purity and crystallinity of the NPs obtained with *L. graveolens*, which probably improves their ability to generate reactive oxygen species (ROS) and alter the permeability of the fungal membrane, key mechanisms in the antifungal activity of ZnO (Chen *et al.*, 2022). On the other hand, the addition of silver to the ZnO NPs enhanced the antifungal capacity at lower concentrations (150 and 250 mg L⁻¹), which indicates a synergistic effect between both metals.

This increase in efficacy at reduced doses could be explained by the ability of Ag to destabilize the fungal cell membrane, interact with thiol groups of proteins, and alter enzymatic functionality, which increases oxidative stress in the fungus (Zhang *et al.*, 2024). In addition, the ZnO/Ag combination was able to generate an improved photocatalytic effect, facilitating the production of free radicals that damage fungal structures, which would explain the more homogeneous control of *A. solani* growth compared to pure ZnO NPs.

Table 2 presents the inhibitory effect of NPs on *A. solani* sporulation, showing a significant reduction in spore production as a function of the concentration applied. The ZnO NPs synthesized with *L. graveolens* extract (ZnO-Lg) showed the most pronounced effect, reducing sporulation by 45% $(3\times10^7\pm0~\text{spores ml}^{-1})$ at 500 mg L⁻¹ compared to the control $(5.57\times10^7\pm0.09~\text{spores lL}^{-1})$.

Table 2. Effect of ZnO and ZnO/Ag nanoparticles on the production of Alternaria solani spores.

Type of nanoparticles	Spores ml-¹			
-	500 mg L-1	1 000 mg L-1		
Control	5.57x10	0 ⁷ ±0.09#		
ZnO-Lg	3x10 ⁷ ±0°	2.44x10 ⁷ ±0.006 ^c		
ZnO-Lt	$3.18 \times 10^7 \pm 0^d$	$2.88 \times 10^7 \pm 0.005^d$		
ZnO-Fc	3.32x10 ⁷ ±0.005 ^e	3.01x10 ⁷ ±0.006 ^e		
Added with silver at 1%				
ZnO/Ag-Lg	$2.37x10^7 \pm 0.02^a$	$1.79 \times 10^7 \pm 0.012^a$		
ZnO/Ag-Lt	2.57x10 ⁷ ±0.01 ^b	2.12X10 ⁷ ±0.023 ^b		
ZnO/Ag-Fc	$2.69 \times 10^7 \pm 0.07^6$	$1.86 \times 10^7 \pm 0.04^a$		

The data represent the mean \pm standard deviation of three independent experiments. Different letters indicate a significant difference according to Tukey's test (p< 0.05). Lg= *Lippia graveolens*, Lt= *Larrea tridentata*, Fc= *Flourensia cernua*.

This effect was intensified at 1 000 mg L⁻¹, reaching a decrease of 56% ($2.44 \times 10^7 \pm 0.006$ spores ml⁻¹), indicating a dose-dependent relationship. Similarly, ZnO NPs synthesized with *L. tridentata* (ZnO-Lt) reduced sporulation by 43% ($3.18 \times 10^7 \pm 0$ spores ml⁻¹) at 500 mg L⁻¹ compared to the control, increasing their efficacy to 49% ($2.88 \times 10^7 \pm 0.005$ spores ml⁻¹) at the highest dose evaluated.

On the other hand, ZnO NPs obtained with *F. cernua* (ZnO-Fc) also demonstrated a significant inhibitory effect, reducing sporulation by 40% (3.32×10^7 ±0.005 spores ml⁻¹) at 500 mg L⁻¹ and achieving a reduction of 45% (3.01×10^7 ±0.006 spores ml⁻¹) at 1 000 mg L⁻¹.

The addition of silver to the ZnO NPs proved to be more effective by reducing the production of *A. solani* spores by a greater percentage (Table 2). ZnO/Ag-Lg NPs exhibited a reduction of 52% $(2.37 \times 10^7 \pm 0.02 \text{ spores mi}^{-1})$ spores at 500 mg L⁻¹ and 68% $(1.79 \times 10^7 \pm 0.012 \text{ spores mi}^{-1})$ at 1 000 mg L⁻¹ compared to the control. Similarly, ZnO/Ag-Lt NPs generated a 54% $(2.57 \times 10^7 \pm 0.01 \text{ spores mi}^{-1})$ reduction of spores at 500 mg L⁻¹, increasing this percentage to 64% at 1 000 mg L⁻¹ $(2.12 \times 10^7 \pm 0.023 \text{ spores mi}^{-1})$. In the same way, ZnO/Ag-Fc NPs showed a 52% reduction in spores at 500 mg L⁻¹, increasing their effect at 1 000 mg L⁻¹ $(1.86 \times 10^7 \pm 0.04 \text{ spores mi}^{-1})$.

It should be noted that the ZnO and ZnO/Ag NPs synthesized by the plant extracts were able to decrease the production of spores as the concentration of the NPs increased; likewise, the addition of silver to zinc oxide favored the increase in the ability to decrease the spores of *A. solani* as the



concentration increased. Statistically, the best treatment for controlling spore production was the one with ZnO/Ag NPs synthesized with *L. graveolens* extract at the two concentrations evaluated (500 and 1 000 mg L⁻¹), which managed to inhibit spore production by 68%.

The results obtained showed that the addition of silver to zinc oxide did not improve in the analysis of the radial growth inhibition test, although it did show a remarkable ability to inhibit spore production. These effects can be explained by the size of the ZnO NPs (<30 nm), as the effectiveness of the NPs is closely related to their size and specific surface area (Nisar *et al.*, 2019). In this case, the concentration of silver at 1% (w/w) turned out to be a limitation in inducing effects on radial growth but favored the reduction in the production of spores of *A. solani*.

This effect can be attributed to the ability of Ag²# ions to accumulate in the fungal cell membrane, penetrate its interior, and interact with the nitrogen bases of DNA, which denatures the genetic material and generates malformations in the hyphae, thus affecting the formation of spores (Rajwade *et al.*, 2020). In this context, the concentration of silver used (1%) in the ZnO/Ag NPs was effective in controlling the sporulation of *A. solani*, although it failed to reduce the radial growth of the fungi significantly.

This finding is consistent with what was reported by Vera-Reyes *et al.* (2019), who noted that 2.5% ZnO/Ag NPs had a greater inhibitory effect on radial growth of *A. solani* compared to pure ZnO NPs. Germinated spores of pathogenic fungi play a crucial role in plant colonization and infection (Ibrahim *et al.*, 2020), so inhibiting spore germination is a key strategy to control the spread of pathogens.

In this sense, the reduction in the germination rate of spores observed in this study highlights the effectiveness of the biosynthesized NPs in mitigating the risks associated with phytopathogenic fungi, which is consistent with other studies that report similar effects (Kriti *et al.*, 2020).

Conclusions

This research showed that the synthesis of nanoparticles (NPs) of ZnO and ZnO/Ag using plant extracts of *Lippia graveolens* (Mexican oregano), *Larrea tridentata* (creosote bush), and *Flourensia cernua* (tarbush) allows us to obtain NPs with a size of less than 30 nm and a high degree of purity. These NPs exhibit a significant antifungal effect against the phytopathogens *Alternaria solani* and *Fusarium oxysporum*, achieving effective control from concentrations of 500 mg L⁻¹. Among the treatments evaluated, NPs synthesized with *L. graveolens* extract showed the highest inhibitory capacity, evidencing a superior effect both in reducing mycelial growth and in decreasing fungal sporulation.

In general, pure ZnO NPs showed a higher percentage of fungal growth inhibition compared to bimetallic NPs (ZnO/Ag), especially at high concentrations, suggesting that the effect of ZnO NPs is sufficient to achieve significant control. Nevertheless, ZnO/Ag NPs showed greater antifungal capacity at low concentrations, reducing the viability of *A. solani* and *F. oxysporum* spores more efficiently, suggesting an initial synergistic effect due to the presence of silver.

Although NPs generated with *L. graveolens* exhibited the best antifungal effect, *L. tridentata* and *F. cernua* extracts also demonstrated significant control over the growth and sporulation of both strains evaluated. The potential of the green synthesis of ZnO and ZnO/Ag NPs as an effective and sustainable strategy for the control of phytopathogenic fungi is highlighted, with promising applications in agriculture for the development of alternative and ecologically friendly biofungicides.

Bibliography

Abdelhakim, H. K.; El#Sayed, E. R. and Rashidi, F. B. 2025. Biosynthesis of zinc oxide nanoparticles with antimicrobial, anticancer, antioxidant and photocatalytic activities by the endophytic *Alternaria tenuissima*. Journal of Applied Microbiology. 128(6):1634-1646. https://dx.doi.org/10.1111/jam.14581.



- Ahmad, H.; Venugopal, K.; Rajagopal, K.; Britto, S.; Nandini, B.; Pushpalatha, H. G.; Konappa, N.; Udayashankar, A. C.; Geetha, N. and Jogaiah, S. 2020. Green synthesis and characterization of zinc oxide nanoparticles using eucalyptus globules and their fungicidal ability against pathogenic fungi of apple orchards. Biomolecules. 10(3):425. https://doi.org/10.3390/biom10030425.
- Ahmad, T.; Xing, F.; Cao, C. and Liu, Y. 2024. Characterization and toxicological potential of *Alternaria alternata* associated with post-harvest fruit rot of Prunus avium in China. Frontiers in Microbiology. 15:1273076. https://doi.org/10.3389/fmicb.2024.1273076.
- 4 Anwar, A.; Masri, A.; Rao, K.; Rajendran, K.; Khan, N. A.; Shah, M. R. and Siddiqui, R. 2019. Antimicrobial activities of green synthesized gums-stabilized nanoparticles loaded with flavonoids. Scientific Reports. 9(1):3122. https://doi.org/10.1038/s41598-019-39528-0.
- Bustillo, P. A. E. 2010. Método para cuantificar suspensiones de esporas de hongos y otros organismos. Universidad Nacional de Colombia. https://doi.org/10.13140/ RG.2.1.3594.5128.
- Chandrasekaran, M. and Paramasivan, M. 2024. Plant growth-promoting bacterial (PGPB) mediated degradation of hazardous pesticides: a review. International Biodeterioration and Biodegradation. 190:105769. https://doi.org/10.1016/j.ibiod.2024.105769.
- 7 Chen, J.; Wu, L.; Song, K.; Zhu, Y. and Ding, W. 2020. Nonphytotoxic copper oxide nanoparticles are powerful "nanoweapons" that trigger resistance in tobacco against the soil-borne fungal pathogen *Phytophthora nicotianae*. Journal of Integrative Agriculture. 21(11):3245-3262. https://doi.org/10.1016/j.jia.2022.08.086.
- Georgekutty, R.; Seery, M. K. and Pillai, S. C. 2008. A highly efficient Ag-ZnO Photocatalyst: synthesis, properties, and mechanism. The Journal of Physical Chemistry C. 112(35):13563-13570. https://doi.org/10.1021/jp802729a.
- Guilger-Casagrande, M. and Lima, R. 2019. Synthesis of silver nanoparticles mediated by fungi: a review. Frontiers in Bioengineering and Biotechnology. 7(287):1-16. Doi: 10.3389/ fbioe.2019.00287.
- Méndez-Andrade, R.; Vallejo-Pérez, M. R.; Loera-Alvarado, E.; Santos-Villarreal, G.; García-Cerda, L. A. and Vera-Reyes, I. 2022. Efficacy of biosynthesized silver nanoparticles from Larrea tridentata against *Clavibacter michiganensis*. Journal of Phytopathology. 170(2):91-99. https://doi.org/10.1111/jph.13058.
- Meng, A.; Sun, S.; Li, Z. and Han, J. 2013. Synthesis, characterization, and dispersion behavior of ZnO/Ag nanocomposites. Advanced Powder Technology. 24(1):224-228. https://doi.org/10.1016/j.apt.2012.06.006.
- Moradi, F.; Sedaghat, S.; Moradi, O. and Arab-Salmanabadi, S. 2021. Review on green nano-biosynthesis of silver nanoparticles and their biological activities: with an emphasis on medicinal plants. Inorganic and Nano-Metal Chemistry. 51(1):133-142. Doi:10.1080/24701556.2020.1769662.
- Muñoz-Ordoñez, I. 2020. Síntesis de nanopartículas de óxido de zinc y óxido de zinc/plata asistida con extractos de *Flourensia cernua* DC: efecto antagónico contra *Clavibacter michiganensis* y en la germinación de semillas de tomate. 17-35 pp. https://ciqa.repositorioinstitucional.mx/jspui/bitstream/1025/625/1/idali%20mu%c3%91oz%20ordo %c3%91ez%20maestria%20en%20ciencias%20en%20agroplasticultura.pdf.
- Nisar, P.; Ali, N.; Rahman, L.; Ali, M. and Shinwari, Z. K. 2019. Antimicrobial activities of biologically synthesized metal nanoparticles: an insight into the mechanism of action. JBIC Journal of Biological Inorganic Chemistry. 24(7):929-941. https://doi.org/10.1007/s00775-019-01717-7.



- Orberá-Ratón, T. M.; Serrat-Díaz, M. J. and González-Giro, Z. 2009. Potencialidades de bacterias aerobias formadoras de endosporas para el biocontrol en plantas ornamentales. Fitosanidad. 13(2):95-100.
- Rajwade, J. M.; Chikte, R. G. and Paknikar, K. M. 2020. Nanomaterials: new weapons in a crusade against phytopathogens. Applied Microbiology and Biotechnology. 104(4):1437-1461. https://doi.org/10.1007/s00253-019-10334-y.
- Rosenberg, M.; Visnapuu, M.; Vija, H.; Kisand, V.; Kasemets, K.; Kahru, A. and Ivask, A. 2020. Selective antibiofilm properties and biocompatibility of nano-ZnO and nano-ZnO/Ag coated surfaces. Scientific Reports. 10:1-15. Doi: 10.1038/s41598-020-70169-w.
- Shireen-Akhter, Q.; Sultana, Z.; Ud-Daula, M. A.; Ashikuzzaman, M. D.; Shamim, R.; Rahman, M. M.; Khaton, A.; Tang, M. A. K.; Rahman, M. S.; Hossain, M. F.; Lee, S. J. and Rahman, A. T. M. M. 2024. Optimization of green silver nanoparticles as nanofungicides for management of rice bakanae disease. Heliyon. 10:e27579. https://doi.org/10.1016/j.heliyon.2024.e27579.
- Vera-Reyes, I.; Esparza-Arredondo, I. J. E.; Lira-Saldívar, R. H.; Granados-Echegoyen, C. A.; Álvarez-Román, R.; Vásquez-López, A.; Santos-Villarreal, G. and Díaz-Barriga, E. 2019. *In vitro* antimicrobial effect of metallic nanoparticles on phytopathogenic strains of crop plants. Journal of Phytopathology. 167(7-8):461-469. https://doi.org/10.1111/jph.12818.
- Zhang, H.; Zheng, T.; Wang, Y., Li, T. and Chi, Q. 2024. Multifaceted impacts of nanoparticles on plant nutrient absorption and soil microbial communities. Frontiers in Plant Science. 15:1-15. Doi:10.3389/fpls.2024.1497006.





Zinc oxide-silver nanoparticles synthesized with plant extracts against Alternaria solani

Journal Information

Journal ID (publisher-id): remexca

Title: Revista mexicana de ciencias agrícolas

Abbreviated Title: Rev. Mex. Cienc. Agríc

ISSN (print): 2007-0934

Publisher: Instituto Nacional de Investigaciones

Forestales, Agrícolas y Pecuarias

Article/Issue Information Date received: 00 May 2025 Date accepted: 00 August 2025 Publication date: 15 October 2025 Publication date: Sep-Oct 2025 Volume: 16

Issue: esp30

Electronic Location Identifier: e4040

DOI: 10.29312/remexca.v16i30.4040

Article Id (other): 00003

Categories

Subject: Articles

Keywords

Keywords

Antifungals zinc nanoparticles zinc-silver nanoparticles

Counts

Figures: 2 Tables: 2 $\quad \textbf{Equations:} \, 0$ References: 20